

Electronic Supplementary Information (ESI)

**Enhanced electrocatalytic Overall Alkaline Water Splitting induced by
Interfacial Electron Coupling of Mn_3O_4 Nano-Cube @ $\text{CeO}_2/\gamma\text{-FeOOH}$
Nanosheet hetero-structure**

Debasish Ghosh,^a Dimple K. Bora,^{b c} Asit Baran Panda^{a b *}

^a Functional Materials Group, Advanced Materials and Corrosion Division, National Metallurgical Laboratory (CSIR-NML), Jamshedpur, Jharkhand, India, 831007.

^b Academy of Scientific & Innovative Research (AcSIR), Ghaziabad, Uttar Pradesh- 201002.

^c Central Salt and marine chemicals research Institute, G B Marg, Bhavnaga, Gujarat, 364002.

Supporting Experimental details.

Synthesis of bare γ -FeOOH:

In a typical synthesis, 100ml distilled water was taken in the 250ml round bottom flask and N₂ was pursed for 5min. Then FeSO₄.7H₂O (0.6 mmol) was added into the flask with continuous stirring in ambient condition. To that solution mixture, hydrazine hydrate (3.6mmol) was added slowly and stirring was continued for 5 min. A greenish black colour suspension was obtained. Then, the nitrogen supply was turned off and constant air flow (20ml/minute) through the solution was started and continued for 5 hours. During air flow the black colour was gradually changed to dark orange colour. Then the solution was centrifuge to collect the suspended materials, washed with water followed by ethanol thoroughly and dried at 60 °C to form γ -FeOOH-NS

Synthesis of bare CeO₂:

In a typical synthesis, 100ml distilled water was taken in the 250ml round bottom flask and N₂ was pursed for 5min. Then Cerium (III) acetate hydrate (0.6 mmol) was added into the flask with continuous stirring in ambient condition. To that solution mixture, hydrazine hydrate (3.6mmol) was added slowly and stirring was continued for 5 min. Then, the nitrogen supply was turned off and constant air flow (20ml/minute) through the solution was started and continued for 5 hours. Then the solution was centrifuged to collect the suspended materials, washed with water followed by ethanol thoroughly and dried at 60 °C to form CeO₂.

Procedure for the calculation of Turnover Frequency (TOF) from OER Current Density.

To ascertain the enhancement of activity post-doping of CeO₂ in Mn₃O₄@ γ -FeOOH, turnover frequencies (TOF) of all catalysts (Mn₃O₄, Mn₃O₄@CeO₂, Mn₃O₄@ γ -FeOOH, and Mn₃O₄@CeO₂/ γ -FeOOH) were calculated. TOF calculation was made utilizing the re-dox area of CV, which provide the electrochemically active atoms present in the catalyst.^{S-1} The respective reduction area is illustrated in Fig. S1. It is evident that the TOF value of Mn₃O₄@CeO₂/ γ -FeOOH (0.603S⁻¹) is better to then the other catalysts Mn₃O₄, Mn₃O₄@CeO₂, Mn₃O₄@ γ -FeOOH (0.0138 S⁻¹, 0.056 S⁻¹, 0.241 S⁻¹). Hence, our foremost active catalyst can produce the number of oxygen molecules compared to our unadorned material per unit time.

In our study, the Turnover Frequency (TOF) was calculated based on the assumption that only the surface-active metal ions, which underwent a redox reaction just prior to the onset of Oxygen evolution reaction (OER), were involved in the OER process. The corresponding expression is:

$$\text{TOF} = (j \times N_A) / (F \times n \times \Gamma) \quad (1)$$

Where, j is the current density, N_A is the Avogadro number, F is the Faraday constant, n is the Number of electrons transferred during the reaction, Γ is the surface concentration of the catalyst.

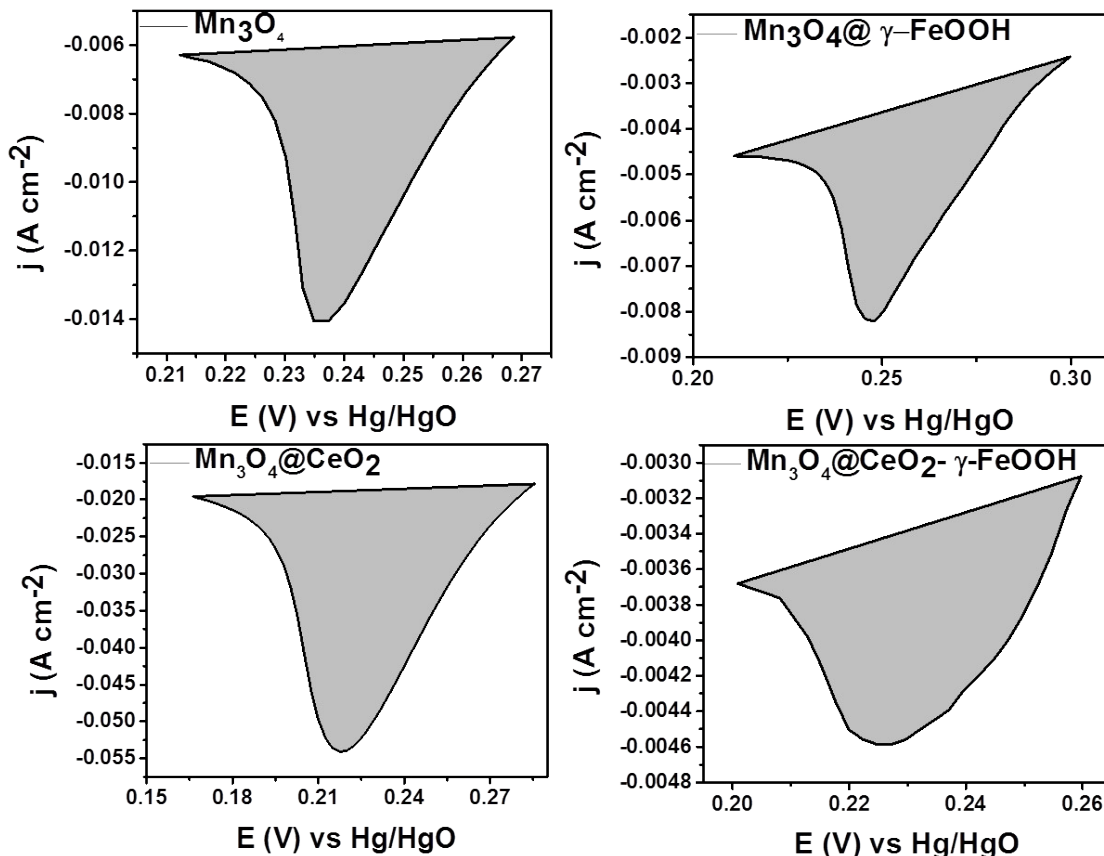


Fig. S1 The area of reduction peaks of the Mn₃O₄, Mn₃O₄@CeO₂, Mn₃O₄@γ-FeOOH and Mn₃O₄@CeO₂/γ-FeOOH.

TOF calculation for Mn₃O₄@CeO₂/γ-FeOOH:

Calculated area associated with the reduction of metal ions of Mn₃O₄@CeO₂/γ-FeOOH = 0.000041440 VA.

$$\begin{aligned} \text{Hence, the associated charge is} &= 0.000041440 \text{ VA} / 0.005 \text{ Vs}^{-1} \\ &= 0.08288 \text{ As} \end{aligned}$$

$$= 0.08288 \text{ C}$$

Now, the number of electron transferred is $= 0.08288 \text{ C} / (1.602 \times 10^{-19} \text{ C})$

$$= 5.17 \times 10^{17}$$

It is anticipated that the reduction a single electron transfer process, the number of electrons involved directly corresponds to the number of surface-active sites.

Hence, the number of M active sites participating in OER is $= 5.17 \times 10^{17}$

Therefore, surface concentration of active sites in the **Mn₃O₄@CeO₂/γ-FeOOH** is 5.17×10^{17} .

The current density at 1.48V potential was evaluated from the backward LSV curve of **Mn₃O₄@CeO₂/γ-FeOOH**.

Hence, from equation (1)

$$\begin{aligned}\text{TOF}_{1.48\text{V}} &= (200 \times 10^{-3}) \times (6.022 \times 10^{23}) / (96485 \times 4 \times 5.17 \times 10^{17}) \\ &= \mathbf{0.603 \text{ s}^{-1}}\end{aligned}$$

Similarly, TOF of other catalyst was also calculated following the identical procedure and the values are as follows.

Catalyst	Turnover Frequency (TOF) _{1.48V}
Mn₃O₄@CeO₂/γ-FeOOH	0.603 s⁻¹
Mn ₃ O ₄ @γ-FeOOH	0.241s ⁻¹
Mn ₃ O ₄ @CeO ₂	0.056s ⁻¹
Mn ₃ O ₄	0.0138s ⁻¹

Procedure for the calculation of Faradaic efficiency of Mn₃O₄@CeO₂/γ-FeOOH.

Faradaic efficiency was calculated using the Eq. (1)

$$\text{Faradaic efficiency} = \frac{\text{experimental } \mu\text{mol of O}_2 \text{ gas}}{\text{theoretical } \mu\text{mol of O}_2 \text{ gas}} \times 100 \quad (1)$$

The theoretical amount of O₂ gas was calculated using Faraday's laws.

$$n = \frac{I \times t}{z \times F} \quad (2)$$

$$= \frac{0.5 \times 4500}{4 \times 96484}$$

$$= 5829 \mu\text{mol}$$

Where n = number of mol, I = current in ampere, t = time in second, z = electrons transfer (for OER= 4), and F = Faraday constant (96485 C mol⁻¹).

The theoretical amount of O₂ gas produced in 75 minutes after 1 h activation = 5829 μmol

The experimental amount of gas (H₂+O₂) was evaluated from the water displacement method at ambient temperature and pressure.

Finally, the total number of moles of gas (H₂+O₂) produced in 75 minutes using water displacement is calculated by the Eq.(3) (considering the ideal behaviour of the gas)

$$PV = nRT \quad (3)$$

Where, V = produced volume of gas in litters, T = temperature in Kelvin, and R = 0.0821 L atm./mol.K, the ideal gas constant.

After 1 h of catalyst activation, the total moles of gas produced in 75 minutes using water displacement:

$$(1 \text{ atm})(0.435L) = n (0.0821 \text{ L atm/ mol K}) (298K)$$

$$n = \frac{(1 \text{ atm}) \times (0.435L)}{(0.082 \text{ L atm/ mol K}) \times (308 K)}$$

$$n = 17223 \mu\text{mol}$$

The molar ratio of produced hydrogen and oxygen in the gas mixture is 2:1

Thus, the moles of O₂ in the gas mixture produced in 75 minutes is

$$n O_2 = 17223 \times \frac{1}{3}$$

$$= 5741 \mu\text{mol}$$

$$\text{Faradaic efficiency: } = \frac{5741 \mu\text{mol}}{5829 \mu\text{mol}} \times 100 \\ = 98.4 \%$$

Similarly, the number of moles of gas produced in 75 minutes using water displacement after 50 hour stability:

$$(1 \text{ atm})(0.431\text{L}) = n (0.0821 \text{ L atm/ mol K}) (298\text{K}) \\ n = \frac{(1 \text{ atm}) \times (0.431\text{L})}{(0.082 \text{ L atm/ mol K}) \times (308 \text{ K})} \\ n = 17065 \mu\text{mol}$$

The molar ratio of produced hydrogen and oxygen in the gas mixture is 2:1

Thus, the moles of O₂ in the gas mixture produced in 75 minutes is

$$n_{O_2} = 17065 \times \frac{1}{3} \\ = 5688 \mu\text{mol} \\ \text{Faradaic efficiency: } = \frac{5688 \mu\text{mol}}{5829 \mu\text{mol}} \times 100 \\ = 97.5 \%$$

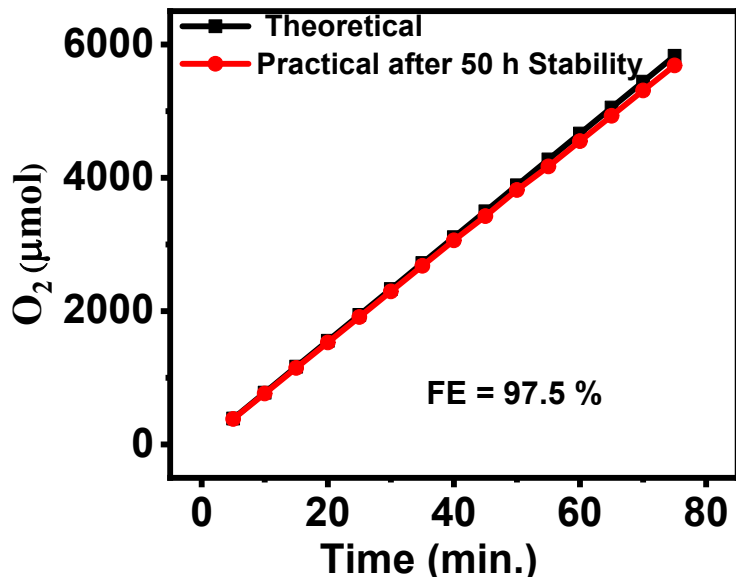


Fig. S2 Theoretical and measured faradaic efficiency after 50 h stability of Mn₃O₄@ CeO₂ / γ-FeOOH.

Other Supporting Figures.

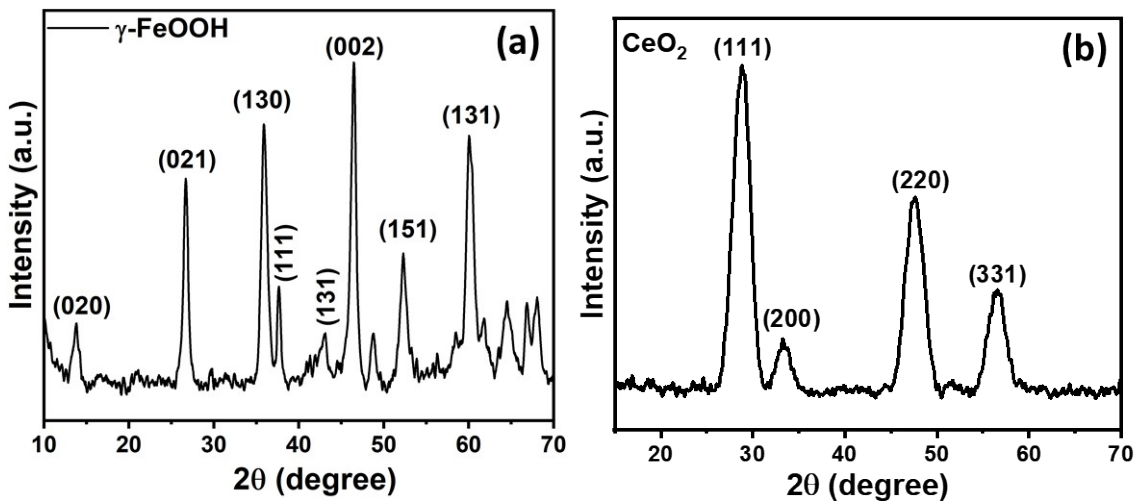


Fig. S3 XRD pattern of bare γ -FeOOH and CeO_2 synthesized in absence of Mn-acetate, the precursor of Mn_3O_4 . The synthesis was performed following identical condition of Mn_3O_4 synthesis.

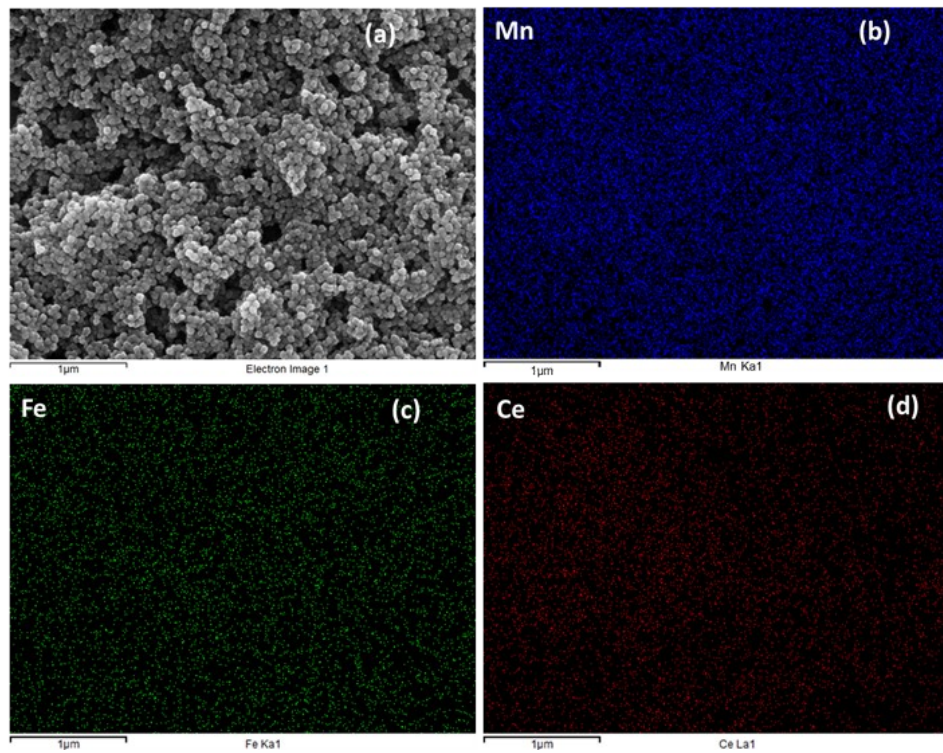


Fig. S4 EDX elemental mapping of the synthesized $\text{Mn}_3\text{O}_4@\text{CeO}_2/\gamma\text{-FeOOH}$ nanocubes.

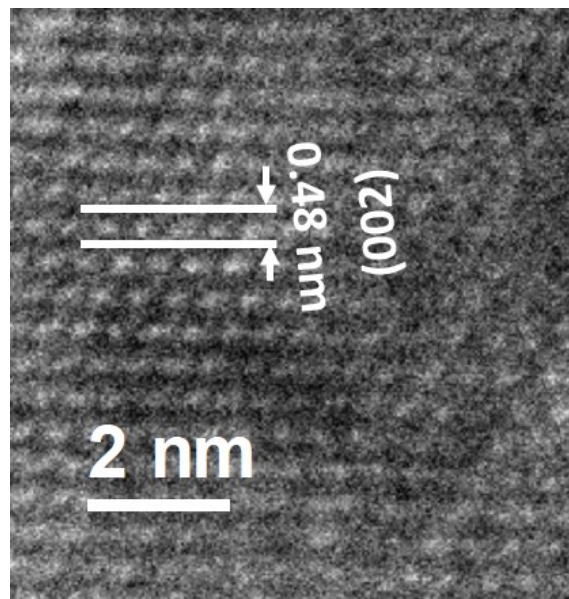


Fig. S5 HR-TEM image of Mn₃O₄ nanocube.

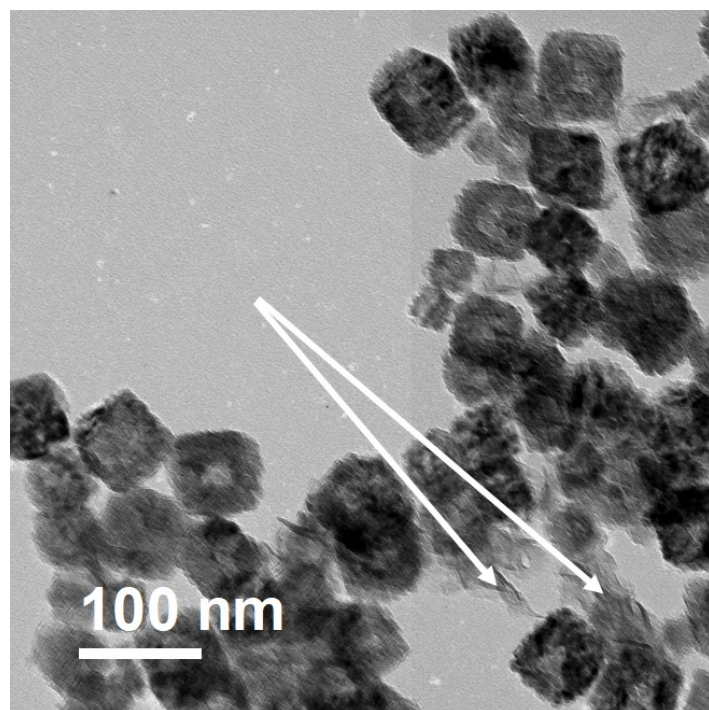


Fig. S6 TEM images of Mn₃O₄@CeO₂/γ-FeOOH indicating the formation of γ-FeOOH nanosheet outside of Mn₃O₄ nanocubes in addition to surface of the cubes. The fringe structure

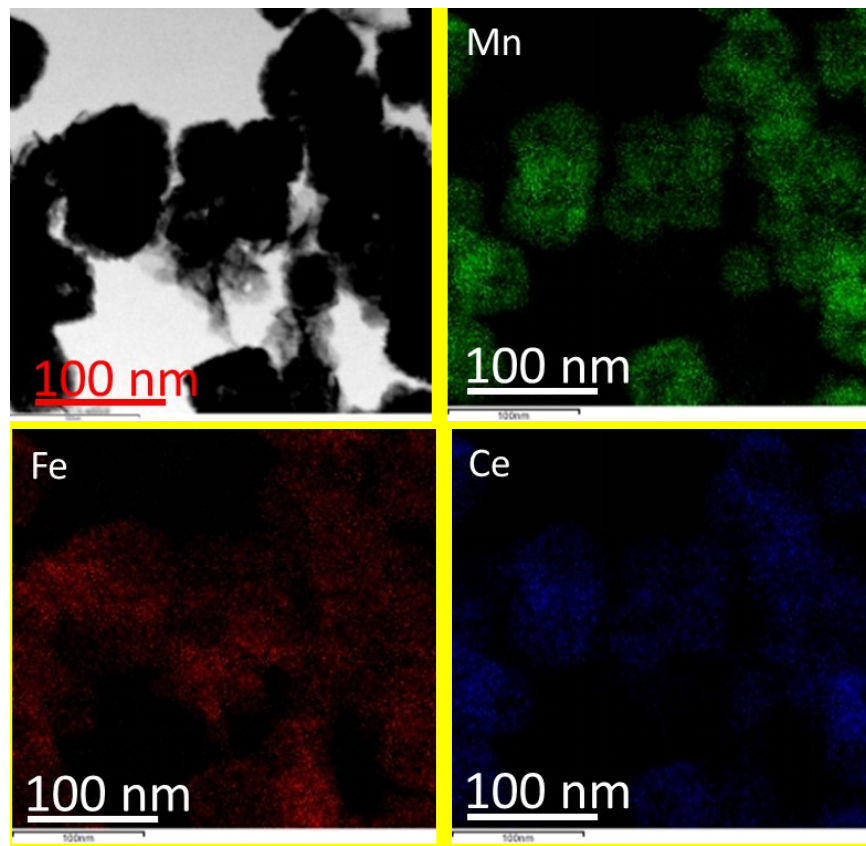


Fig. S7 TEM EDX elemental mapping images of $\text{Mn}_3\text{O}_4@\text{CeO}_2/\gamma\text{-FeOOH}$

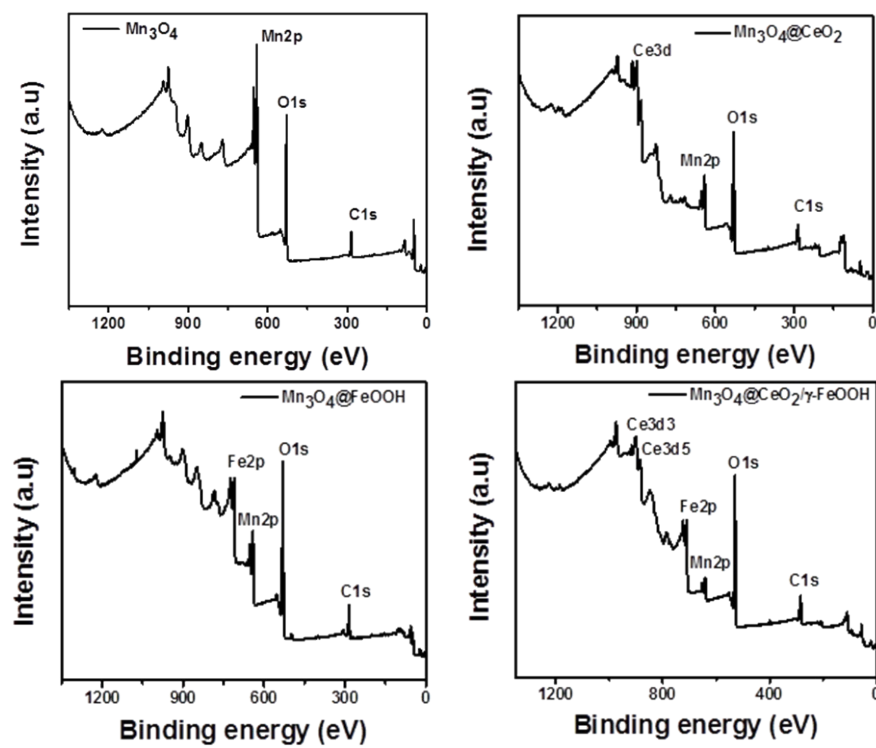


Fig. S8 XPS survey spectra of different samples.

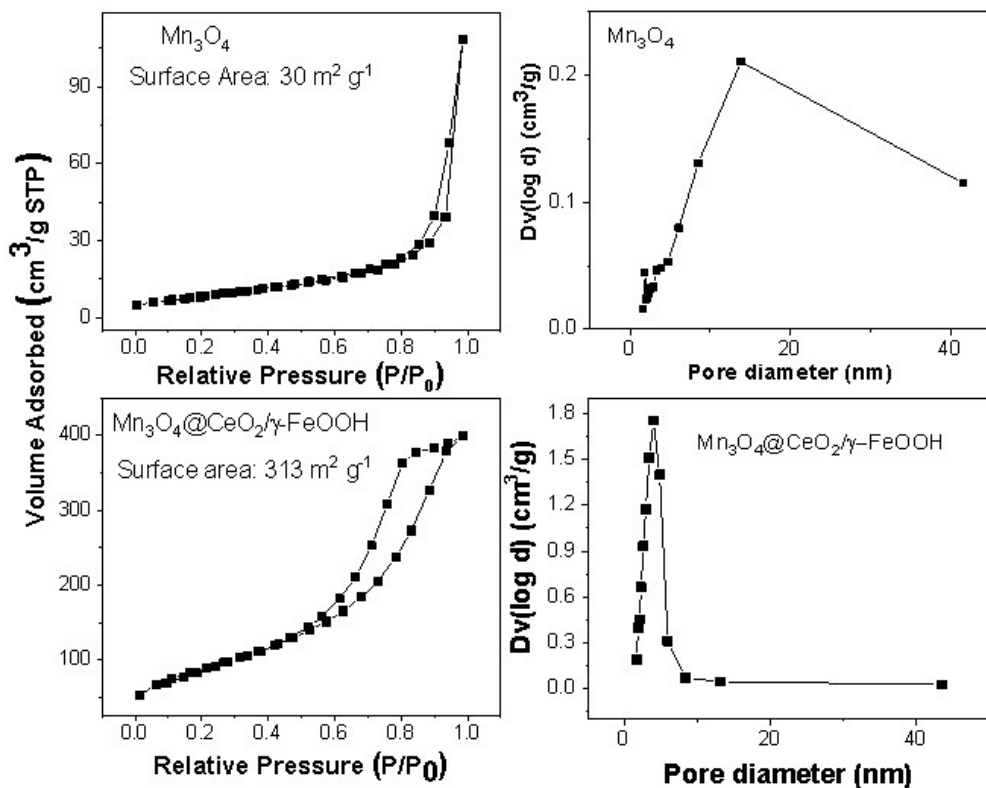


Fig. S9 The nitrogen adsorption desorption isotherm and respective pore size distribution of the synthesized bare Mn_3O_4 nano-cube and $\text{Mn}_3\text{O}_4@\text{CeO}_2/\gamma\text{-FeOOH}$ nanocomposite.

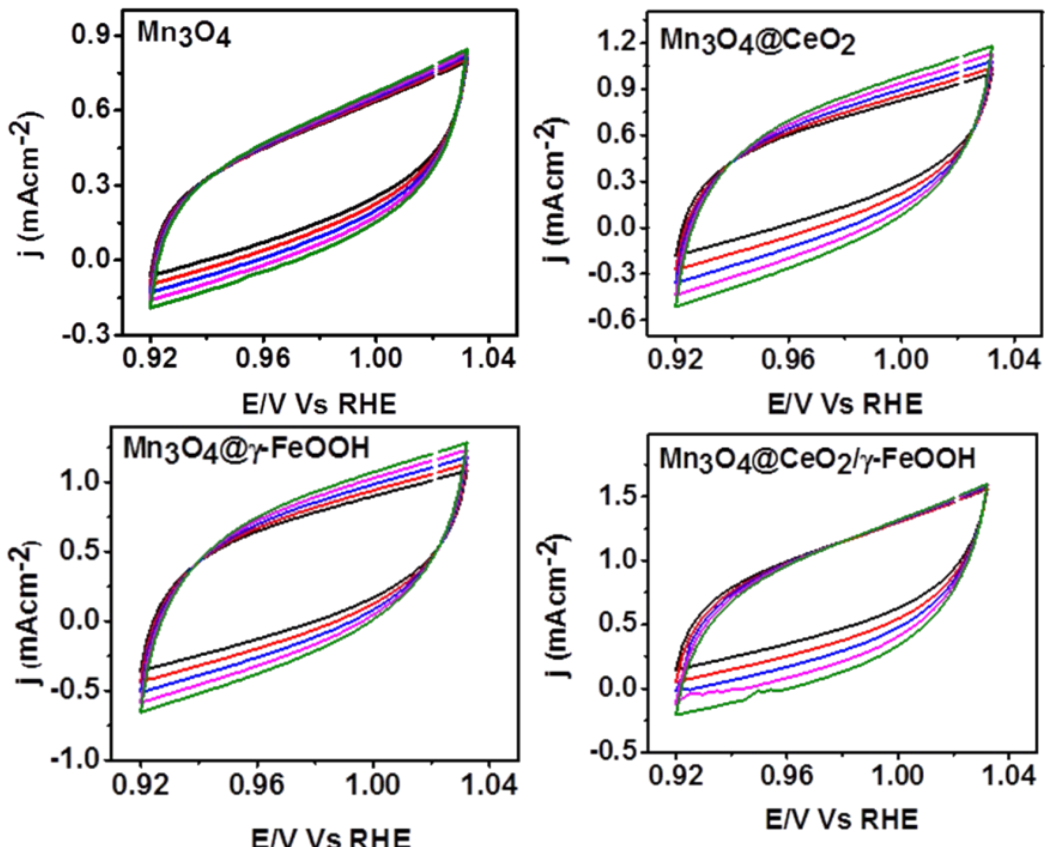


Fig. S10 CV curves at varying scans rate of 50, 60, 70, 80, 90 mV S^{-1} of different samples.

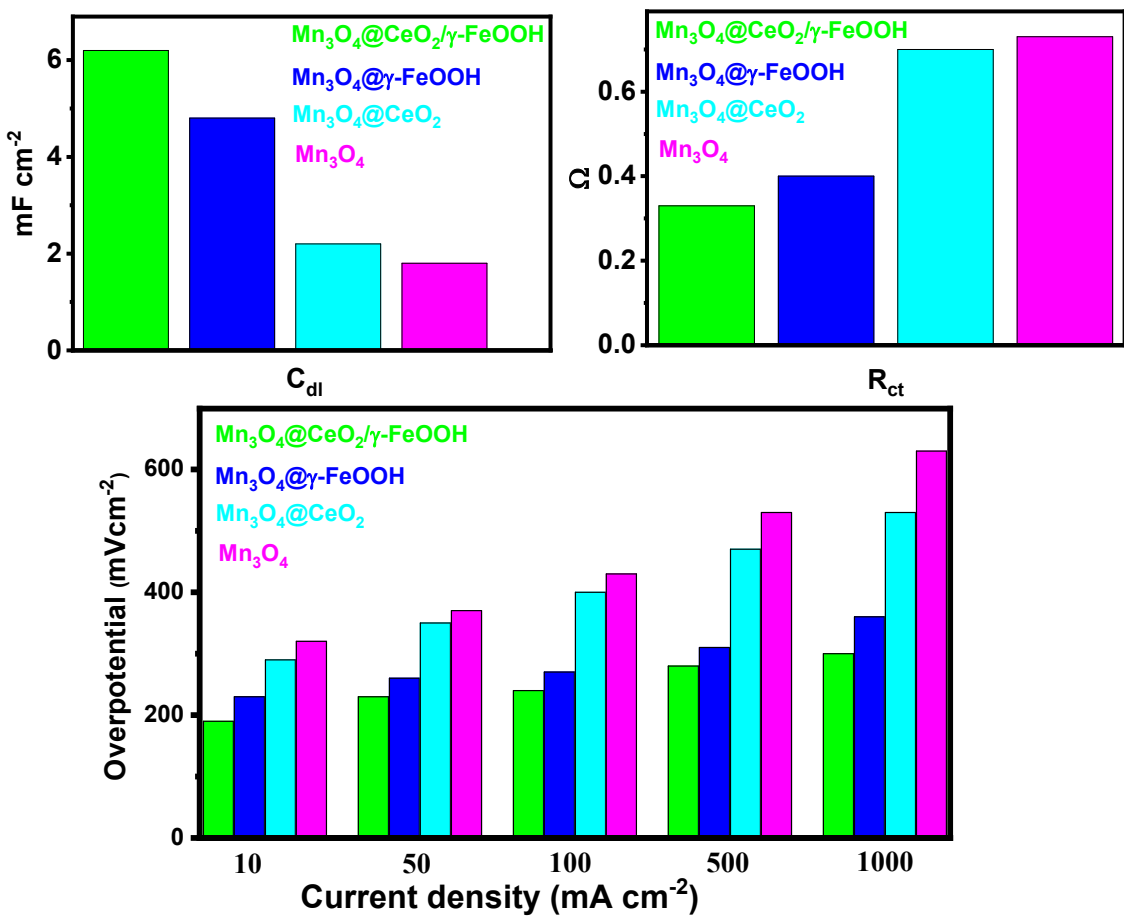


Fig. S11 Summarized OER performances of all the tested samples in bar diagram.

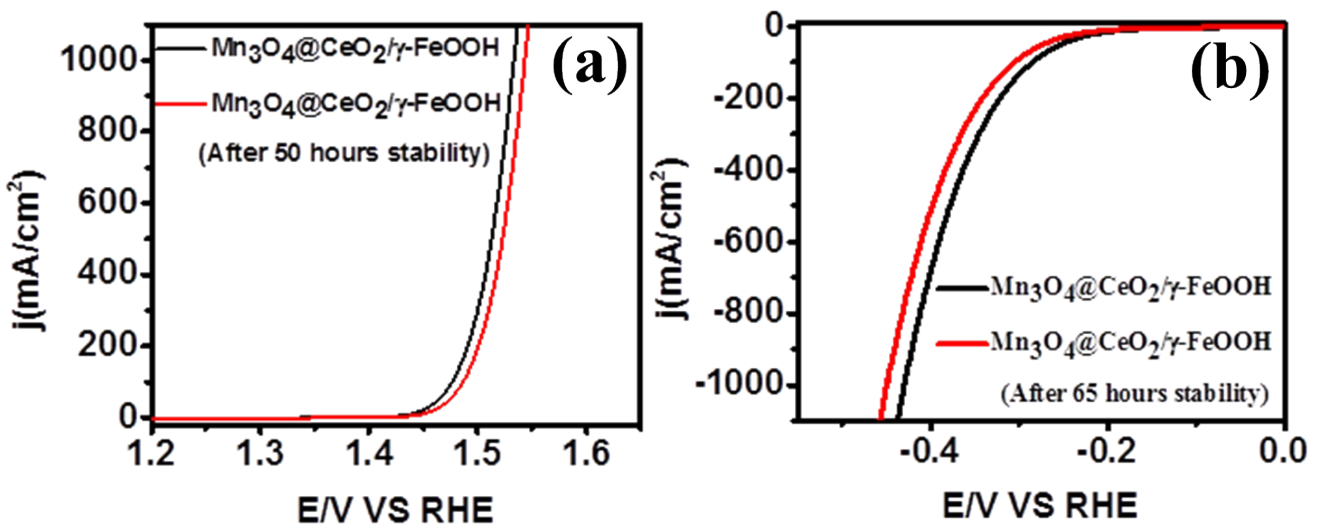


Fig. S12 LSV after and before stability a) OER b) HER.

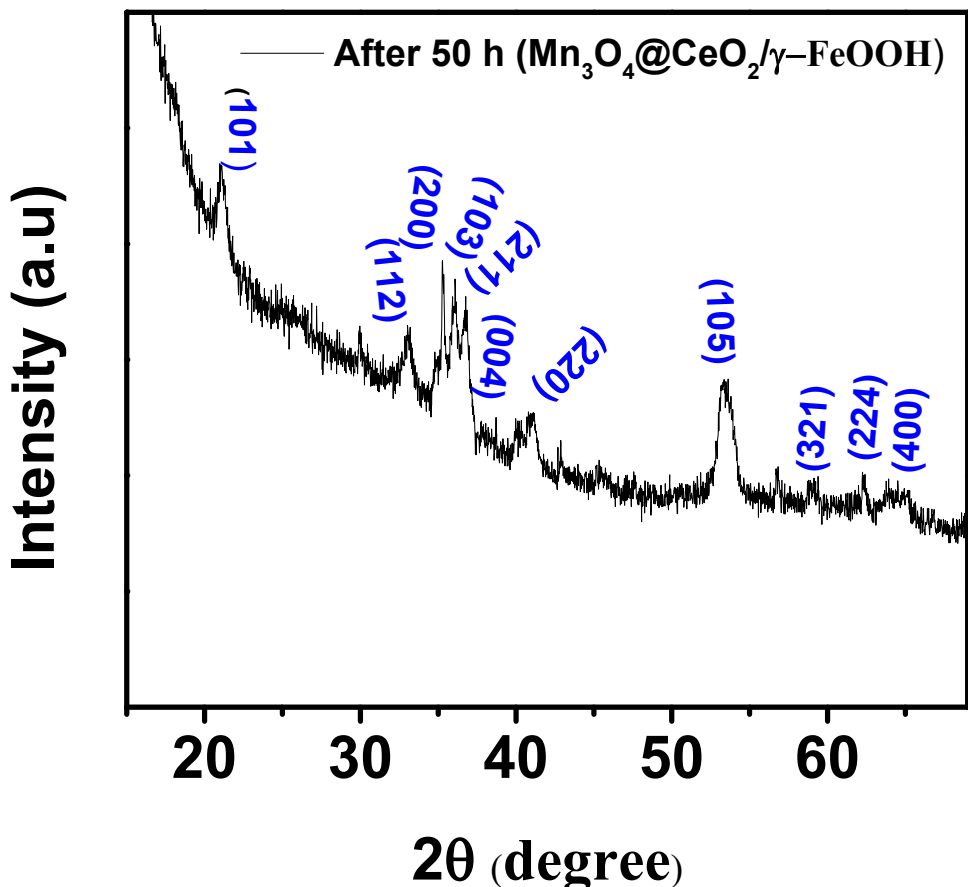


Fig. S13 XRD pattern of $\text{Mn}_3\text{O}_4@\text{CeO}_2/\gamma\text{-FeOOH}$ after 50h of chronopotentiometry experiment at 1.53 V to attain a current density of 1000mA cm^{-2} .

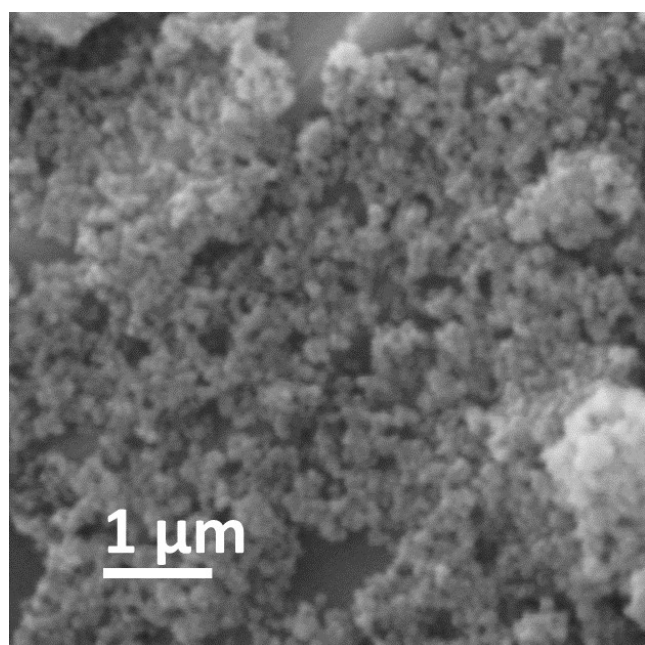


Fig. S14 SEM image of $\text{Mn}_3\text{O}_4@\text{CeO}_2/\gamma\text{-FeOOH}$ after 50h of chronopotentiometry experiment at 1.53 V to attain a current density of 1000mA cm^{-2} .

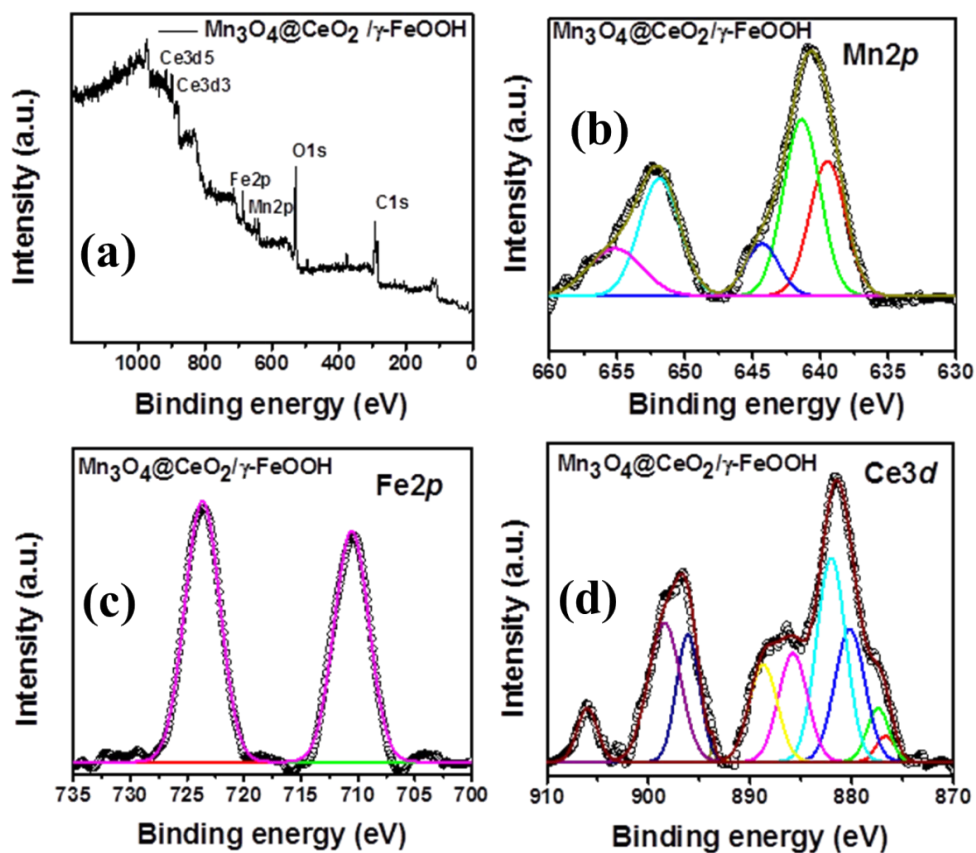


Fig. S15 XPS spectra of $\text{Mn}_3\text{O}_4@\text{CeO}_2/\gamma\text{-FeOOH}$ after 50h of chronopotentiometry experiment at 1.53 V to attain a current density of 1000 mA cm^{-2} .

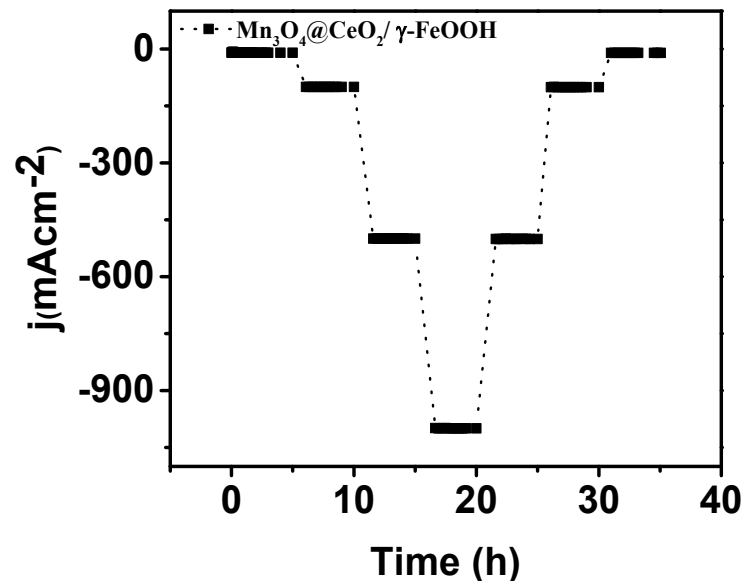


Fig. S16 HER chronoamperometric measurement as a function of different current densities of $\text{Mn}_3\text{O}_4@\text{CeO}_2/\gamma\text{-FeOOH}$.

Supporting Tables

Table S1. Comparison of the OER activities of $\text{Mn}_3\text{O}_4@\text{CeO}_2/\gamma\text{-FeOOH}$.

Electrocatalyst	Electrolyte	η_{10} Overpotential (mV)	η_{100} Overpotential (mV)	η_{500} Overpotential (mV)	Tafel (mV dec ⁻¹)	References
$\text{Mn}_3\text{O}_4@\text{CeO}_2/\gamma\text{-FeOOH}$	1M KOH	190	240	280	34	This work
MnFeO-NF-0.2	1M KOH	227	274	295		S-2
MnFeO-NF-0.4	1M KOH	157	225	257		S-2
MnFeO-NF-0.6	1M KOH	220	285	312		S-2
MnFeO-NF-0.8	1M KOH	243	319	356		S-2
MnFeO-NF-1	1M KOH	258	340	405		S-2
$\text{MnO}_2\text{-NF}$	1M KOH	342	433	464		S-2
$\text{Mn}_3\text{O}_4\text{-NF}$	1M KOH	339	438	481		S-2
$\text{Fe}_2\text{O}_3\text{-NF}$	1M KOH	318	432			S-2
$\text{Co}_{0.85}\text{Se/NC}$	1M KOH		406		93	S-3
Ce-NiCoP/NF	1M KOH		282		52.3	S-4
Mo–NiCoP/C	1M KOH		364		76.7	S-5
Mo-NiCoP/NF	1M KOH		326		49.4	S-6
$\text{Co}(\text{Ni})\text{O}_x@\text{CoP}_{x-3}$	1M KOH		479		108.4	S-6
$\text{Ni}_2\text{P}-\text{CoCH}/\text{CFP}$	1M KOH		320		36	S-8
ho-LaNi ₅ /NF	1M KOH		347		82	S-9
Co-CoO/Ti ₃ C ₂ -MXene	1M KOH	196	400		47	S-10
Ni–W–P@HFC	1M KOH		380		88.3	S-11

FeMnZn/Mn-FeS	1M KOH		390			S-12
Cu(OH) ₂ /Cu	1M KOH		390			S-13
MCo ₂ O ₄ @MCo ₂ S ₄ @ PPy	1M KOH		395			S-14
CuO NCA	1M KOH		400			S-15
Pd	1M KOH		400			S-16
N-FeP	1M KOH		440			S-17
Fe ₇ S ₈ /NGF	1M KOH		450			S-18
Ni ₂ Mo ₃ N/NF	1M KOH		392			S-19
MoSe ₂ -Ni ₃ Se ₂ /NF	1M KOH		395			S-20
CoFe-LDH /CoFe ₂ O ₄ /NF	1M KOH		400			S-21

Table S2. Comparison of the HER activities of **Mn₃O₄@CeO₂/γ-FeOOH**

Electrocatalyst	Electrolyte	η_{10} Overpotential (mV)	η_{20} Overpotential (mV)	References
Mn₃O₄@CeO₂/γ-FeOOH	1M KOH	180	190	This Work
FeMnZn/Mn-FeS	1M KOH		118	S-12
Fe _{1-x} CoxS ₂ /CNT	1M KOH		120	S-22
NiOx NPs	1M KOH		174	S-23
Co ₂ P	1M KOH		171	S-24
CNTs@NiP ₂ /NiP	1M KOH		137	S-25
FeCoNi- LTH/NiCo ₂ O ₄ /CC	1M KOH		151	S-26
Cu@Cu ₂ S	1M KOH		203	S-27

VC-NS	1M KOH		120	S-28
MoP/Mo ₂ N	1M KOH		165	S-29
Co ₂ P	1M KOH		167	S-30
Ni(OH) ₂	1M KOH		170	S-31
m-NiS _{x-0.5} /NF	1M KOH		137	S-32
Ni-NiO/N-rGO	1M KOH		160	S-33
CoS _x -Ni ₃ S ₂ /NF	1M KOH		146	S-34
Ni ₃ S ₂ /Co ₃ S ₄	1M KOH		150	S-35
NiCo ₂ O ₄	1M KOH		160	S-36
Co-B/Ni	1M KOH		200	S-37
Co ₃ O ₄ /MoS ₂	1M KOH		221	S-38

Table S3. Comparison of the overall water splitting performance of reported catalysts.

Catalyst	Electrolyte	Potential	Current density	Reference
Mn ₃ O ₄ @CeO ₂ /γ-FeOOH	1M KOH	1.55 V	10 mAcm ⁻²	This work
FeMnZn/Mn-FeS	1M KOH	1.62 V	10 mAcm ⁻²	S-12
NF	1M KOH	1.65 V	10 mAcm ⁻²	S-39
Ni ₃ Se ₂	1M KOH	1.65 V	10 mAcm ⁻²	S-40
xNiP@SS	1M KOH	1.77 V	10 mAcm ⁻²	S-41
CoP@NF CoP/CoO@NF	1M KOH	1.62 V	10 mAcm ⁻²	S-42
CoP/VGNHs	1M KOH	1.63 V	10 mAcm ⁻²	S-43
CoS ₂ /CC	1M KOH	1.66 V	10 mAcm ⁻²	S-44
Co ₂ N/TM/Co-Pi/TM	1M KOH	1.78 V	10 mAcm ⁻²	S-45
Co _{0.4} Fe _{0.6} LDH/g-	1M KOH	1.61 V	10 mAcm ⁻²	S-46

CNx				
CoFe@N-GCNCs-700	1M KOH	1.63 V	10 mAcm ⁻²	S-47
CoFe ₂ O ₄	1M KOH	1.63 V	10 mAcm ⁻²	S-48
CoNiN@NiFe LDH	1M KOH	1.63 V	10 mAcm ⁻²	S-49
CuFe Composite	1M KOH	1.64 V	10 mAcm ⁻²	S-50
NiCo ₂ O ₄	1M KOH	1.65 V	10 mAcm ⁻²	S-51
FeCoS/C	1M KOH	1.66 V	10 mAcm ⁻²	S-52
DLD-FeCoP@CNT	1M KOH	1.67 V	10 mAcm ⁻²	S-53
Ni-Co-S/CF	1M KOH	1.67 V	10 mAcm ⁻²	S-54
NiMoP ₂	1M KOH	1.67 V	10 mAcm ⁻²	S-55
FeCoP	1M KOH	1.68 V	10 mAcm ⁻²	S-56
Ni/MoN@NCNT/CC	1M KOH	1.69 V	10 mAcm ⁻²	S-57
NiS/MoS ₂	1M KOH	1.69 V	10 mAcm ⁻²	S-58
NiCo ₂ O ₄	1M KOH	1.72 V	10 mAcm ⁻²	S-59
Cu ₂ S-Ni ₃ S ₂	1M KOH	1.77 V	10 mAcm ⁻²	S-60
Co-Fe binary oxide	1M KOH	1.92 V	10 mAcm ⁻²	S-61
Ni-Fe-Doped K0.23MnO ₂	1M KOH	1.62 V	10 mAcm ⁻²	S-62
Fe-Ni-Cr	1M KOH	1.64 V	10 mAcm ⁻²	S-63
Te/Fe-NiOOH	1M KOH	1.65 V	10 mAcm ⁻²	S-64
Fe-Ni2P/MoS _x /NF	1M KOH	1.68 V	10 mAcm ⁻²	S-65
FexNiy/CeO ₂	1M KOH	1.70 V	10 mAcm ⁻²	S-66
CoFeNiO	1M KOH	1.96 V	10 mAcm ⁻²	S-67
Co _{0.85} Se/NC	1M KOH	1.7	10 mAcm ⁻²	S-68

Table S4. Comparison of the AEM electrolyzer performance with relevant literature

Catalyst	Electrolyte	Potential (2V) Current density (mAcm ⁻²)	Reference
Mn₃O₄@CeO₂/γ-FeOOH AEM Mn₃O₄@CeO₂/γ-FeOOH	1M KOH	366	This Work
Pt/C AEM IrO ₂	1M KOH	101	This Work
NiCoTi/Ti AEM NiCoTi/Ti	1M KOH	180	S69
NiCo/r-GO AEM Co ₃ O ₄ /r-GO	1M KOH	105	S70
CuCoO AEM Ni	1M KOH	156	S71
Cu _x Co _{3-x} O ₄ AEM Ni	1M KOH	100	S72
NiCo ₂ O ₄ /Ni AEM Ni	1M KOH	106	S73
γ-FeOOH-NS AEM γ-FeOOH- NS	1M KOH	209	S74

References.

- S1. S. S. Roy, A. Karmakar, R. Madhu, S. Nagappan, H. N Dhandapani and S. Kundu, *ACS Appl. Energy Mater.*, 2023, **6**, 8818-8829.
- S2. J. Luo, W. H. Guo, Q. Zhang, X. H. Wang, L. Shen, H. C. Fu, L. L. Wu, X. H. Chen, H. Q. Luo and N. B. Li, *Nanoscale*, 2020, **12**, 19992-20001.
- S3. W.-W. Tian, Y.-D. Ying, J.-T. Rena and Z.-Y. Yuan, *J. Mater. Chem. A.*, 2023, **11**, 8024-8037.
- S4. T. Zhao, G. Xu, B. Gong, J. Jiang and L. Zhang, *Nano Res.*, 2024, **17**, 282-289.
- S5. J. Lin, Y. Yan, C. Li, X. Si, H. Wang, J. Qi, J. Cao, Z. Zhong, W. Fei and J. Feng, *Nano-Micro Lett.*, 2019, **11**, 55.
- S6. Y. Zhao, J. Chen, S. Zhao, W. Zhou, R. Dai, X. Zhao, Z. Chen , T. Sun, H. Zhang and A. Chen, *J. Alloys Compd.*, 2022, **918**, 165802.
- S7. T. Zhang, X. Ren, F. Ma, X. Jiang, Y. Wen, W. He, L. Hao, C. Zeng, H. Liu, R. Chen, H. Zhang and H. Ni, *Appl. Mater. Today*, 2023, **34**, 101912.
- S8. S. Zhang, C. Tan, R. Yan, X. Zou, F.-L. Hu, Y. Mi, C. Yan and S. Zhao, *Angew. Chem. Int. Ed.*, 2023, **62**, 202302795.
- S9. Y. Wu, Y. Liu, K. Liu, L. Wang, L. Zhang, D. Wang, Z. Chai and W. Shi, *Green Energy Environ.*, 2022, **7**, 799-806.
- S10. D. Guo, X. Li, Y. Jiao, H. Yan, A. Wu, G. Yang, Y. Wang, C. Tian and H. Fu, *Nano Res.*, 2022, **15**, 238-247.
- S11. T. Li, H. Chen, Z. Chen, Z. Xue, X. Zhang, and B. Hui, *ACS Sustain Chem Eng.*, 2023, **11**, 14549- 14558.
- S12. L. Huang, R. Yao, Z. Li, J. He, Y. Li, H. Zong, S. Han, J. Lian, Y.-G. Li and X. Ding, *Green Chem.*, 2023, **25**, 4326-4335.
- S13. P. Babar, A. Lokhande, V. Karade, B. Pawar, M. G. Gang, S. Pawar and J. H. Kim, *J. Colloid Interface Sci.*, 2019, **537**, 43-49.
- S14. D. Zhao, H. Liu and X. Wu, *Nano Energy*, 2019, **57**, 363-370.
- S15. W.-L. Xiong, M. I. Abdullah and M.-M. Ma, *Chin. J. Phys.*, 2018, **31**, 806-812.
- S16. K. S. Joya, M. A. Ehsan, N.-U.-A. Babar, M. Sohail and Z. H. Yamani, *J. Mater. Chem. A*, 2019, **7**, 9137-9144.
- S17. M. Yang, J.-Y. Xie, Z.-Y. Lin, B. Dong, Y. Chen, X. Ma, M.-L. Wen, Y.-N. Zhou, L. Wang and Y.-M. Chai, *Appl. Surf. Sci.*, 2020, **507**, 145096.
- S18. X. Huang, S. Wang, X. Zhang and L. Liu, *Int. J. Electrochem. Sci.*, 2021, **16**, 210433.
- S19. S. H. Park, S. H. Kang and D. H. Youn, *Materials*, 2021, **14**, 4768.

- S20. Y. Liu, Y. Liu, Y. Yu, C. Liu and S. Xing, *Front. Energy res.*, 2022, **16**, 483-491.
- S21. Z. Guo, X. Wang, F. Yang and Z. Liu, *J. Alloy. Compd.*, 2022, **895**, 162614.
- S22. H. Li, S. Chen, H. Lin, X. Xu, H. Yang, L. Song and X. Wang, *Small*, 2017, **13**, 1701487.
- S23. Z. Huang, Z. Chen, Z. Chen, C. Lv, M. G. Humphrey and C. Zhang, *Nano Energy*, 2014, **9**, 373-382.
- S24. S. Singh, D. C. Nguyen, N. H. Kim and J. H. Lee, *Chem. Eng. J.*, 2022, **442**, 136120.
- S25. Y. Liu, Y. Bai, Y. Han, Z. Yu, S. Zhang, G. Wang, J. Wei, Q. Wu and K. Sun, *ACS Appl. Mater. Interfaces*, 2017, **9**, 36917-36926.
- S26. T. Duy Thanh, H. Van Hien, L. Huu Tuan, N. H. Kim and J. H. Lee, *J. Mater. Chem. A*, 2020, **8**, 14746-14756.
- S27. X. Peng, L. Hu, L. Wang, X. Zhang, J. Fu, K. Huo, L. Y. S. Lee, K.-Y. Wong and P. K. Chu, *Nano Energy*, 2016, **26**, 603-609.
- S28. Y. Gu, A. Wu, Y. Jiao, H. Zheng, X. Wang, Y. Xie, L. Wang, C. Tian and H. Fu, *Angew Chem Int Edit*, 2021, **60**, 6673-6681.
- S29. C. Lv, X. Wang, L. Gao, A. Wang, S. Wang, R. Wang, X. Ning, Y. Li, D. W. Boukhvalov, Z. Huang and C. Zhang, *ACS Catal.*, 2020, **10**, 13323-13333.
- S30. F. Jing, Q. Lv, J. Xiao, Q. Wang and S. Wang, *J. Mater. Chem. A*, 2018, **6**, 14207-14214.
- S31. X. Liu, W. Liu, M. Ko, M. Park, M. G. Kim, P. Oh, S. Chae, S. Park, A. Casimir, G. Wu and J. Cho, *Adv. Funct. Mater.*, 2015, **25**, 5799-5808.
- S32. L. Jiang, N. Yang, C. Yang, X. Zhu, Y. Jiang, X. Shen, C. Li and Q. Sun, *Appl. Catal., B*, 2020, **269**, 118780.
- S33. H. Su, S. Song, S. Li, Y. Gao, L. Ge, W. Song, T. Ma and J. Liu, *Appl. Catal., B*, 2021, **293**, 120225.
- S34. X. Gao, H. Zhang, Q. Li, X. Yu, Z. Hong, X. Zhang, C. Liang and Z. Lin, *Angew Chem Int Edit*, 2016, **55**, 6290-6294.
- S35. W. Hao, R. Wu, R. Zhang, Y. Ha, Z. Chen, L. Wang, Y. Yang, X. Ma, D. Sun, F. Fang and Y. Guo, *Adv. Energy Mater.*, 2018, **8**, 1801372.
- S36. A. Muthurasu, V. Maruthapandian and H. Y. Kim, *Appl. Catal., B*, 2019, **248**, 202-210.
- S37. J. Hu, C. Zhang, L. Jiang, H. Lin, Y. An, D. Zhou, M. K. H. Leung and S. Yang, *Joule*, 2017, **1**, 383-393.
- S38. Y. Hou, M. R. Lohe, J. Zhang, S. Liu, X. Zhuang and X. Feng, *Energy Environ. Sci.*, 2016, **9**, 478-483.
- S39. R. Ding, S. Cui, J. Lin, Z. Sun, P. Du and C. Chen, *Catal. Sci. Technol.*, 2017, **7**, 3056-3064.
- S40. J. Shi, J. Hu, Y. Luo, X. Sun and A. M. Asiri, *Catal. Sci. Technol.*, 2015, **5**, 4954-4958.

- S41. A. Z. Alhakemy, A. B. A. A. Nassr, A. E.-H. Kashyout and Z. Wen, *Sustainable Energy and Fuels*, 2022, **6**, 1382-1397.
- S42. B. Qiu, A. Han, D. Jiang, T. Wang and P. Du, *ACS Sustain. Chem. Eng.*, 2019, **7**, 2360- 2369.
- S43. T. Linh, S.-K. Jerng, S. B. Roy, J. H. Jeon, K. Kim, K. Akbar, Y. Yi and S.-H. Chun, *ACS Sustain. Chem. Eng.*, 2019, **7**, 4625-4630.
- S44. W. Fang, D. Liu, Q. Lu, X. Sun and A. M. Asiri, *Electrochem. Commun.*, 2016, **63**, 60-64.
- S45. L. Zhang, L. Xie, M. Ma, F. Qu, G. Du, A. M. Asiri, L. Chen and X. Sun, *Catal. Sci. Technol.*, 2017, **7**, 2689-2694.
- S46. T. Bhowmik, M. K. Kundu and S. Barman, *ACS Appl. Energy Mater.*, 2018, **1**, 1200.
- S47. H.-J. Niu, Y.-P. Chen, R.-M. Sun, A.-J. Wang, L.-P. Mei, L. Zhang and J.-J. Feng, *J. Power Sources*, 2020, **480**, 229107.
- S48. B. Debnath, S. Parvin, H. Dixit and S. Bhattacharyya, *Chemsuschem*, 2020, **13**, 3875-3886.
- S49. J. Wang, G. Lv and C. Wang, *Appl. Surf. Sci.*, 2021, **570**, 151182.
- S50. A. I. Inamdar, H. S. Chavan, B. Hou, C. H. Lee, S. U. Lee, S. Cha, H. Kim and H. Im, *Small*, 2020, **16**, 1905884.
- S51. X. Gao, H. Zhang, Q. Li, X. Yu, Z. Hong, X. Zhang, C. Liang and Z. Lin, *Angew Chem Int Edit*, 2016, **55**, 6290-6294.
- S52. W. Wang, Y. Xu, J. Yao, X. Liu, Z. Yin and Z. Li, *Dalton Trans.*, 2020, **49**, 13352-13358.
- S53. B. Wang, Y. Chen, Q. Wu, Y. Lu, X. Zhang, X. Wang, B. Yu, D. Yang and W. Zhang, *J. Mater. Sci. Technol.*, 2021, **74**, 11-20.
- S54. T. Liu, X. Sun, A. M. Asiri and Y. He, *Int. J. Hydrogen Energy*, 2016, **41**, 7264-7269.
- S55. X.-D. Wang, H.-Y. Chen, Y.-F. Xu, J.-F. Liao, B.-X. Chen, H.-S. Rao, D.-B. Kuang and C.-Y. Su, *J. Mater. Chem. A*, 2017, **5**, 7191-7199.
- S56. K. L. Sun, K. H. Wang, T. P. Yu, X. Liu, G. X. Wang, L. H. Jiang, Y. Y. Bu and G. W. Xie, *Int. J. Hydrogen Energy*, 2019, **44**, 1328-1335.
- S57. P. Wang, J. Qi, C. Li, X. Chen, T. Wang and C. Liang, *Chemelectrochem*, 2020, **7**, 00023.
- S58. Y. Zheng, P. Tang, X. Xu and X. Sang, *J. Solid State Chem.*, 2020, **292**, 121644.
- S59. R. Zhao, D. Cui, J. Dai, J. Xiang and F. Wu, *Sustain. Mater. Techno.*, 2020, **24**, e00151.
- S60. K. S. Bhat and H. S. Nagaraja, *Chemistryselect*, 2020, **5**, 2455-2464.
- S61. W. Adamson, X. Bo, Y. Li, B. H. R. Suryanto, X. Chen and C. Zhao, *Catal. Today*, 2020, **351**, 44-49.
- S62. H. Liao, X. Guo, Y. Hou, H. Liang, Z. Zhou and H. Yang, *Small*, 2020, **16**, 1905223.
- S63. J. Zhang, H. Jang, L. L. Chen, X. L. Jiang, M. G. Kim, Z. X. Wu, X. Liu and J. Cho, *Mater. Chem. Phys.*, 2020, **241**, 122375.

- S64. S. Ibraheem, X. T. Li, S. S. A. Shah, T. Najam, G. Yasin, R. Iqbal, S. Hussain, W. Y. Ding and F. Shahzad, *ACS Appl. Mater. Interfaces*, 2021, **13**, 10972-10978.
- S65. X. L. Zhang, C. Liang, X. Y. Qu, Y. F. Ren, J. J. Yin, W. J. Wang, M. S. Yang, W. Huang and X. C. Dong, *Adv. Mater. Interfaces*, 2020, **7**, 1901926.
- S66. L. Chen, H. Jang, M. G. Kim, Q. Qin, X. Liu and J. Cho, *Inorg. Chem. Front.*, 2020, **7**, 470-476.
- S67. Y. He, D. Aasen, A. McDougall, H. Yu, M. Labbe, C. Ni, S. Milliken, D. G. Ivey and J. G. C. Veinot, *Chemelectrochem*, 2021, **8**, 1391-1392.
- S68. W.-W. Tian, Y.-D. Ying, J.-T. Ren and Z.-Y. Yuan, *J. Mater. Chem. A.*, 2023, **11**, 8024-8037.
- S69. P. Anesan, A. Sivanantham, and S. Shanmugam, *ACS Appl. Mater. Interfaces*, 2017, **14**, 12416–12426
- S70. S. Kamali, M. Zhiani and H. Tavakol, *Renew Energ.*, 2020, **154**, 1122-1131
- S71. E. Lopez-Fernandez, J. Gil-Rostra, C. Escudero, I. J. Villar-Garcia, F. Yubero, A. D. Consuegra and A. R. Gonzalez-Elipe, *J. Power Sources*, 2021, **485**, 229217
- S72. E. Lopez-Fernandez, J. Gil-Rostra, J. P. Espinos, A. R. Gonzalez-Elipe, F. Yubero and A. de Lucas-Consuegra, *J. Power Sources*, 2019, **415** 136-144.
- S73. D. Chanda, J. Hnat, T. Bystron, M. Paidar and K. Bouzek, *J. Power Sources*, 2017, **347**, 247-258.
- S74 D. K. Bora, D. Ghosh, A. Jana, R. K. Nagarale, and A. B. Panda, *ACS Appl. Eng. Mater.*, 2024, **2**, 975-987.